



Pre-normative REsearch for Safe use of
Liquid Hydrogen (PRESLHY)

Fuel Cells and Hydrogen Joint Undertaking (FCH 2 JU)

Grant Agreement Number 779613

Summary of experiment series E4.1 results (Ignition parameters)

Deliverable Number:	4.4 (D21)
Version	1.0
Author(s):	C. Proust, INERIS
Submitted Date:	25 July 2019 and 28/03/2021
Due Date:	30 November 2018
Report Classification:	Confidential



**FUEL CELLS AND HYDROGEN
JOINT UNDERTAKING**

History		
Nr.	Date	Changes/Author
1.0	25.7.2019	Original version by C. Proust/INERIS

Approvals			
Version	Name	Organisation	Date

Key words

Cryogenic temperature, flowing mixture, minimum ignition energy, hot surface ignition, laminar flame propagation and explosion

Acknowledgements, Preface and Disclaimer

The PRESLHY project has received funding from the Fuel Cells and Hydrogen 2 Joint Undertaking under the European Union's Horizon 2020 research and innovation programme under grant agreement No 779613.

The test program for the investigation of the ignition properties of a cryogenic hydrogen-air flow was split into two parts. The first is devoted to the ignition of flowing (up to 30 m/s) and cold (down to -130°C) hydrogen-air mixtures and the second to the spark ignition of the same mixtures. Given the very touchy aspects associated to controlling very weak electrical sparks, requiring a highly controlled atmosphere, the same apparatus could not be used for both measurement series.

After some preliminary field tests, it was decided to run the hot surface ignition tests in the open atmosphere outside using a large sort of wind tunnel. The spark energy measurements will be done in a transparent vessel in a laboratory. The flowing aspect will be dropped since ignition is immediate so that for the ignition process, the atmosphere is still. The possibility for the initial flame kernel to spread out in the flow is a distinct flame propagation problem.

For MIE measurements, a new type of spark generator, enabling a very good control of the energy delivered into the spark, was designed. It was tested with various mixtures. To do the experiment, a special burner was designed containing glass beads. The latter can be cooled down to cryogenic temperature by pouring liquid nitrogen before flowing the flammable mixture through it. MIE of hydrogen air mixtures were measured between ambient temperature and -120°C. As expected, MIE increases as the temperature drops. The evolution of the flammability limits with the temperature was also investigated.

This report contains the “meta data” of the respective experiments, providing description of the experimental set-up, sensors and results. Detailed evaluation of the results, as well as any modelling work is excluded here and left for subsequent work.

Despite the care that was taken while preparing this document the following disclaimer applies: The information in this document is provided as is and no guarantee or warranty is given that the information is fit for any particular purpose. The user thereof employs the information at his/her sole risk and liability.

The document reflects only the authors’ views. INERIS and the European Union are not liable for any use that may be made of the information contained therein.

Publishable Short Summary

About 500 experiments were performed with the facilities described in this report, varying the hydrogen concentration in air %H₂ (between 4 and 75%), the flow velocity U (0 to 35 m/s) and the temperature of the mixture T⁰ (ambient to -130 °C). Note that the later temperature is the lowest that can be achieved in a jet of LH₂ and air at the upper flammability limit.

The device used to measure the hot surface temperature (T_{pcrit}) is a straight horizontal tube, 10 cm diameter, 2.5 m long equipped with a flange in which gaseous hydrogen, gaseous nitrogen, gaseous oxygen and when required liquid nitrogen are admitted and mixed. This arrangement enables to vary independently %H₂, U and T⁰. The hot body is a nichrome wire spiralled around a 10 mm alumina core. It is electrically heated and the temperature can be varied.

The device used to measure the minimum ignition energy (MIE) is a burner. A special spark generator was developed and tested. A significant effort was devoted to its development and to the control of the spark. Even with this well controlled apparatus, not more than half of the stored energy is retrieved in the spark gap. It is claimed that significant progresses have been made in the estimate of MIE since the overlap between the “no ignition” event and the “ignition” event is usually within a factor of two whereas in other apparatus it might spread over a factor of 10 or 100 of the results. No statistics were required here.

A surprising result was obtained which was not expected. T_{pcrit} does not vary with %H₂, U and T⁰ and is close to 600°C, very close to the autoignition temperature (AIT). For standard hydrocarbons, T_{pcrit} is much larger than the AIT. MIE is seen to increase in a less than linear manner when the temperature decreases.

Table of Contents

Key words.....	ii
Acknowledgements, Preface and Disclaimer.....	ii
Publishable Short Summary	iv
1 Purpose of the Tests – Knowledge Gap Addressed.....	1
2 Measurement of T_{pcrit} for LH₂ releases.....	1
2.1 Hardware and measurements	1
2.2 Results.....	4
3 Measurement of MIE for cold H₂-air mixtures	6
3.1 Generating a very cold H ₂ -air mixture	6
3.2 Spark generator	8
3.3 MIE measurements.....	14
3.4 LFL-UFL measurements	17
4 Conclusions	17

1 Purpose of the Tests – Knowledge Gap Addressed

In the work package WP4.1 of the PRESLHY project, the fundamental ignition parameters of hydrogen air mixtures issued from a release of LH₂ have to be measured. To the knowledge of the present authors, this has never been done before.

In a former project, INERIS had the opportunity to measure the temperature and concentration in the plume resulting from an atmospheric release of LH₂. It can be shown that the lowest temperature in the flammable zone reached at the upper flammability limit is 100 K so -170°C. This is the lowest temperature that we targeted in this project. The maximum velocity is that which could be obtained in the jet under a few bars overpressure at the upper flammability limit and is not more than 30 m/s.

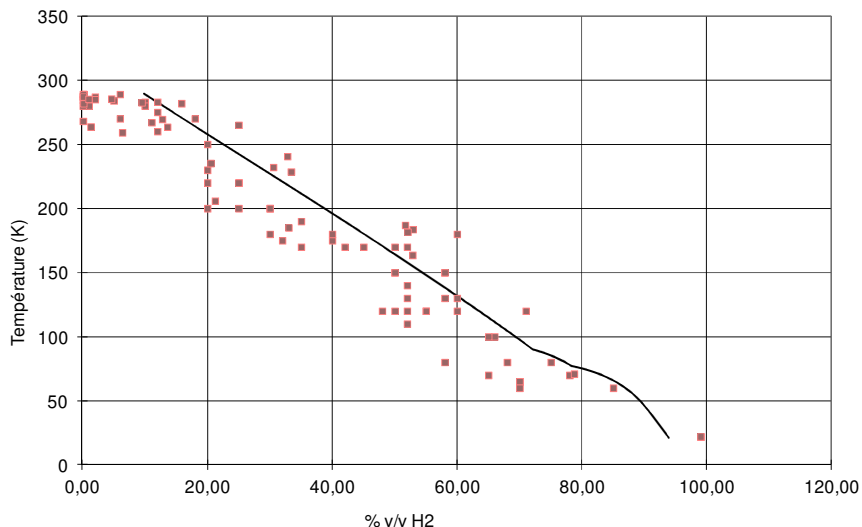


Figure 1: measurement of %H₂ and associated temperature in a plume resulting from an atmospheric release (free jet) of LH₂

Therefore, to measure these fundamental ignition parameters for LH₂, original setups were designed. They differ significantly. The setups and the results for MIE and T_{pcrit} will then be presented in two separate chapters.

2 Measurement of T_{pcrit} for LH₂ releases

2.1 Hardware and measurements

The mixture is continuously flowing in a constant diameter tube (0.1 m inner diameter, 2.5 m long) equipped with a double envelope to ensure thermal insulation (figure 2a). To vary flexibly the composition of the atmosphere and its temperature, gaseous nitrogen, gaseous oxygen, gaseous hydrogen and liquid nitrogen are injected via calibrated ports (figure 2b) in the flange of the pipe. The injection of liquid nitrogen allows reducing the temperature of the flammable atmosphere. The typical overpressure ahead of the calibrated ports is a few bars insuring a high injection velocity. It was checked that perfect homogeneity was achieved at 1 m from the flange. The flowrate is regulated using high flowrate pressure regulators (figure 2c), carefully calibrated, but as explained later, the composition and temperature of the atmosphere is controlled at the exit of the pipe. All the flammable range could be explored with velocities ranging from nearly zero (0.5 m/s) to 30 m/s and temperature between -120°C to ambient.

*a- General view**b- Injection ports*

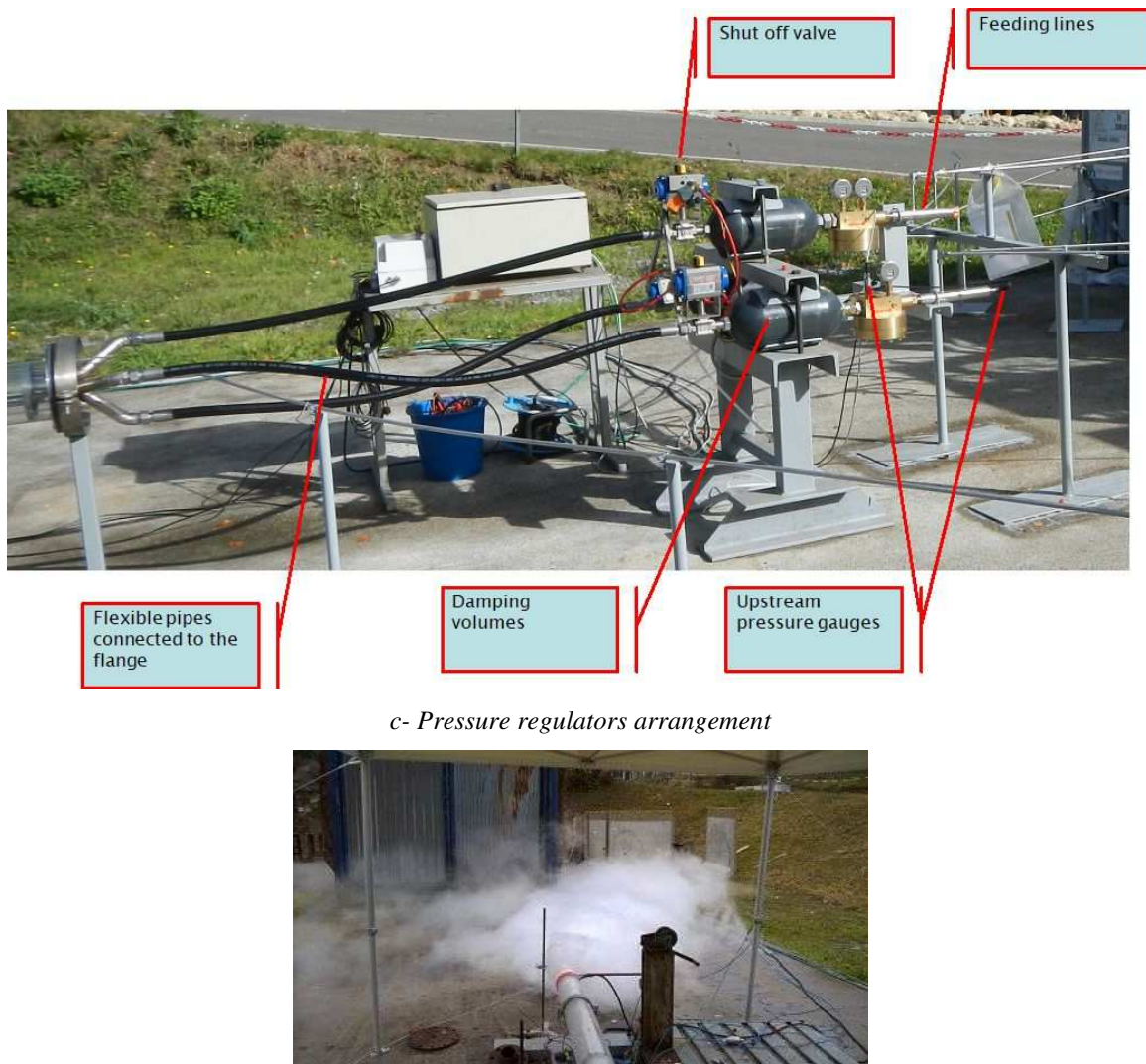


Figure 2: Details of the setup for Tpcrit measurements

The ignition source is an electrically heated coil (Figure 3). It is a 0.7 m long, 0.8 mm diameter nichrome wire, tightly spiralled around a 9 mm diameter, 30 mm long alumina core.

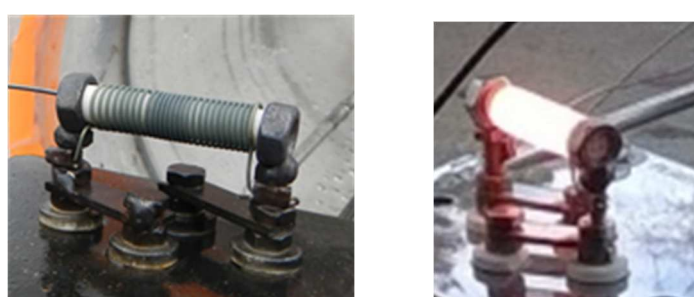


Figure 3 : hot coil arrangement (0.7 m nichrome wire 0.8 mm diameter spiralled over a 9 mm diameter 30 mm long alumina cylinder) – electrically heated

It was carefully calibrated using a laboratory 2 colour pyrometer coupled with a field infrared camera (FLIR) also used during the field experiments. The temperature of the coil

is rather homogeneous (Figure 4) and a very accurate reading of the temperature can be obtained with the infrared camera. It is believed the accuracy of the measurement is about $\pm 30^\circ\text{C}$ (at 700°C).

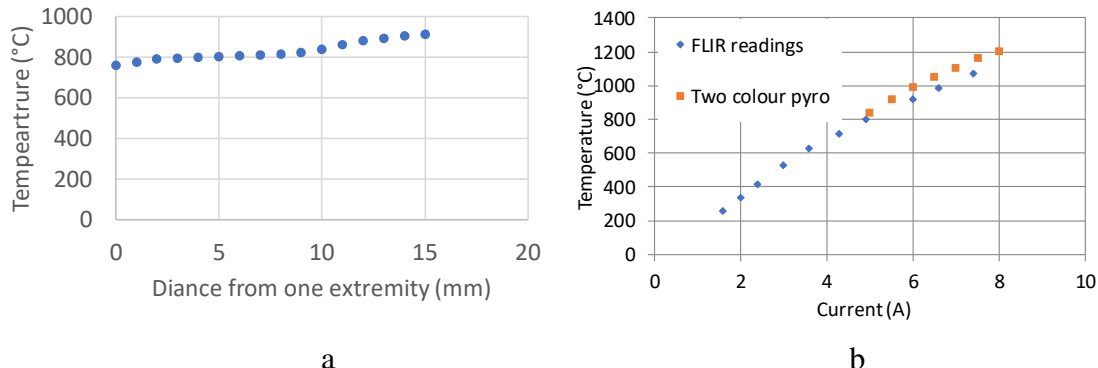


Figure 4: Two-colour pyrometer calibration (a) and comparison with field measurement infrared camera (b)

The hot coil is inserted inside the pipe in the centre of the open-end cross section.

The temperature of the atmosphere is measured using a sleeved (0.5 mm diameter) K thermocouple (accuracy on the order of $\pm 1^\circ\text{C}$) inserted 10 cm upstream from the open-end cross section. The oxygen concentration is measured at the same point using paramagnetic oxygen cells (accuracy $\pm 0.01\%\text{O}_2$ v/v). The hydrogen concentration is deduced, and the expected accuracy of this measurement is $\pm 0.1\%\text{H}_2$ v/v.

The temperature of the coil is measured using the infrared camera.

The pressures upstream of the pressure regulators are controlled using 0-200 bar Kistler gauges (accuracy ± 0.1 bar). The flow velocity is deduced from the calibration curves of the pressure regulators and of temperature of the atmosphere (to estimate the quantity of LN₂ injected when used and the specific mass of the mixture). The accuracy of this estimation is not better than $\pm 10\%$.

The ignition is usually obvious, but an additional K thermocouple is installed 2 cm downstream from the hot coil.

To run an experiment, the flowrates of oxygen and nitrogen are first established, and the oxygen concentration is measured to ensure the mixture mimics air. Then hydrogen is admixed to reach the targeted oxygen content in the mixture. Then the coil is slowly heated up until ignition. A typical experiment lasts 15 min.

2.2 Results

The first point is about the influence of the reactivity of the mixture (figure 5). Given the uncertainty of the measurement of the temperature of the hot coil, the influence of the reactivity seems very small. The critical hot surface ignition temperature is smaller than found up to now (870K) but is coherent with the suspected influence of the size of the hot body. Note also that this temperature is very close to the auto-ignition temperature.

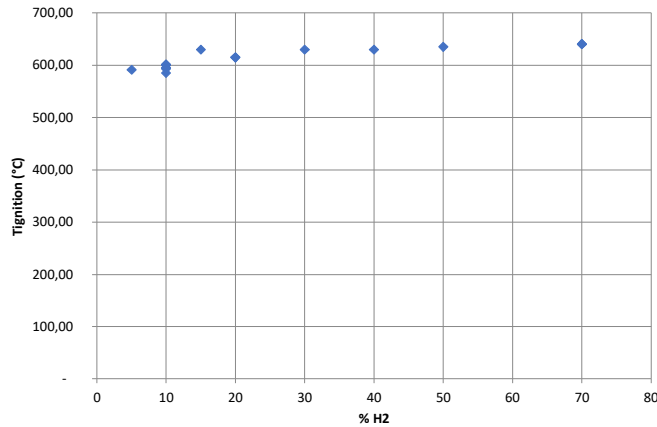


Figure 5: Influence of the proportion of H₂ in the mixture on the hot surface ignition temperature (ambient conditions and at rest)

The second point is about the influence of the temperature of the flammable atmosphere. The data of figure 6 were established for 10% H₂-air mixtures because for this composition, the hot surface ignition temperature is the lowest and the ignition event is clear (more difficult to judge with leaner mixtures). Again, the influence is not detectable which is in line with the predictions given the measurement uncertainties.

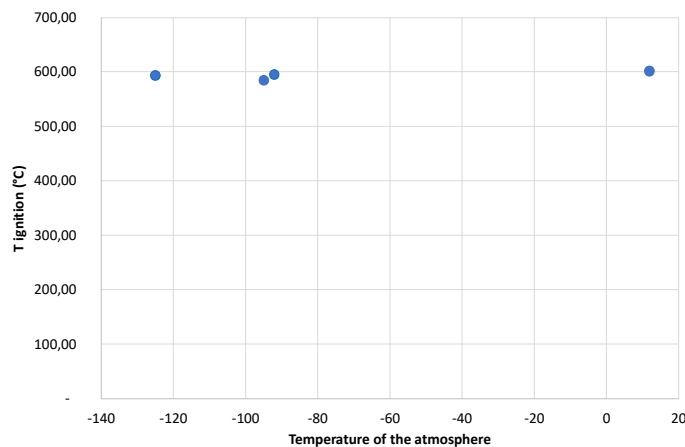


Figure 6: Influence of the temperature of the H₂ air mixture on the hot surface ignition temperature (10% H₂ at rest)

The last point is about the influence of the velocity of the flammable atmosphere. The data of figure 7 were established for 10% H₂-air mixtures at ambient conditions. The influence is hardly detectable. If any, the influence is far less than postulated.

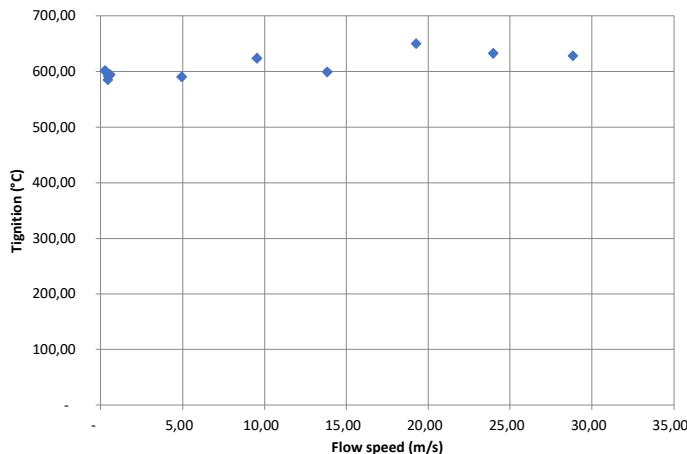


Figure 7: Influence of the velocity of the H₂ air mixture on the hot surface ignition temperature (10 % H₂, ambient conditions)

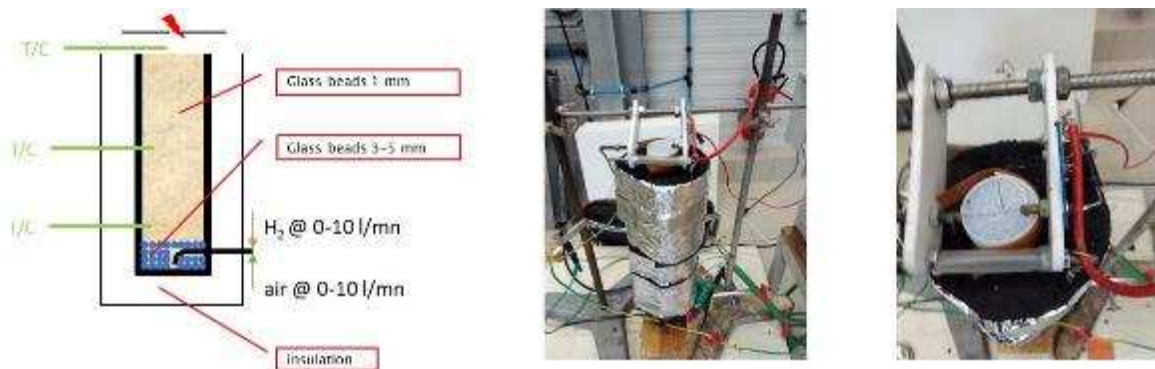
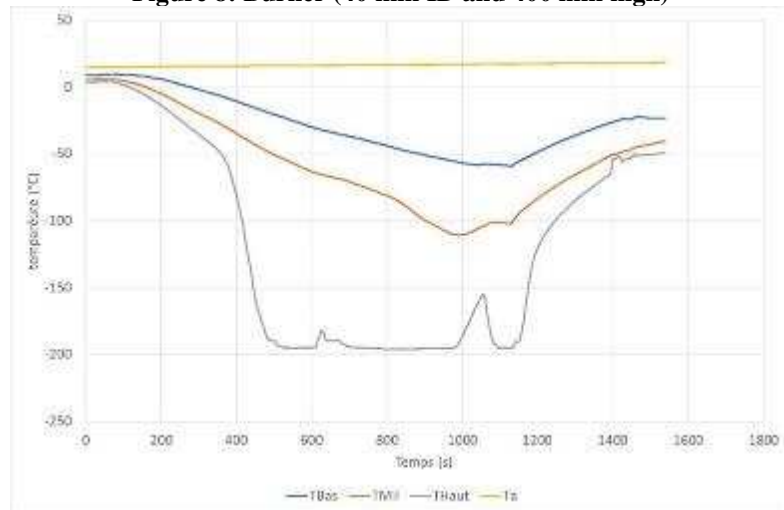
3 Measurement of MIE for cold H₂-air mixtures

Spark ignition is an instantaneous process so that at the time scale of the ignition period the flow is always still. There is thus no need to produce a flowing mixture. The spreading of the initial flame kernel to the rest of the flammable cloud is a flame propagation problem.

3.1 Generating a very cold H₂-air mixture

Initially, it was planned to use a closed bomb method so that not only the MIE could be measured but also, during the same tests, the flame propagation and explosion characteristics. Attempts were done as shown in the appendix 1 and they were successful at ambient temperature for propane. However, for hydrogen air mixture, the method was difficult to handle due to humidity condensing on the electrodes and was nearly impossible to adapt to very low temperatures.

An alternative method was designed. A burner was devised (figure 8). It is a vertical metallic tube (40 mm diameter and about 400 mm high) filled with glass beads. Three 0.5 mm thermocouple (K type) are inserted into the bed: at the bottom, in the middle and at the top. It is thermally insulated using a special foam. The flammable mixture is introduced from the bottom and diffuses upwards. Ignition is produced just above the surface and the bed of particles quenches the flame. When cooled mixtures are desired the bed is cooled before the ignition tests by pouring about 2 liters of liquid nitrogen from the top. A typical temperature time curve is shown on figure 9. There is time for about 30 min of test at reduced temperature.


Figure 8: Burner (40 mm ID and 400 mm high)

Figure 9: Temperature evolution into the bed of glass beads after pouring 2 l of liquid nitrogen

The mixture is prepared using calibrated mass flowmeters (figure 10). The composition was checked using a paramagnetic oxygen meter (SERVOMEX : O₂% accuracy = $\pm 0.1\%$ v/v) to ensure that the ratio of the flowrate gives an accurate estimate of the real gaseous composition, provided the mass flowmeters are operated in between 10% and 90% of the full regulation range. It is believed that the accuracy of the measurement of the concentration is $\pm 0.5\%$ v/v. It was further verified that the hydrogen concentration is constant over the cross section of the burner and up to some cm above.



Figure 10: Mass flowmeter arrangement for hydrogen-air experiments (0-10 l/min each)

3.2 Spark generator

In the spark gap, a part of the electrical energy is dissipated into heat which is the source of the ignition. But part of it is lost in producing the conditions sustaining the current stream (vaporizing the material of the electrodes, anode/cathode EMF,...), heat conduction towards the electrodes, shock waves, thermal radiation,... Small tungsten electrodes are a good mean for reducing the first two sources of losses whereas a better control of the current and duration of the spark is required to reduce the two last sources of losses which supposes a flexible control of the current/voltage supply. The spark gap layout is shown on figure 11. The electrodes are 0.3 mm in diameter (Tungsten), tightly screwed on steel rods in such a way that any heat loss sources (supports, walls) are cm away from the spark gap. The spark gap is fixed to 0.5 mm and is carefully controlled all along the experimental campaign.

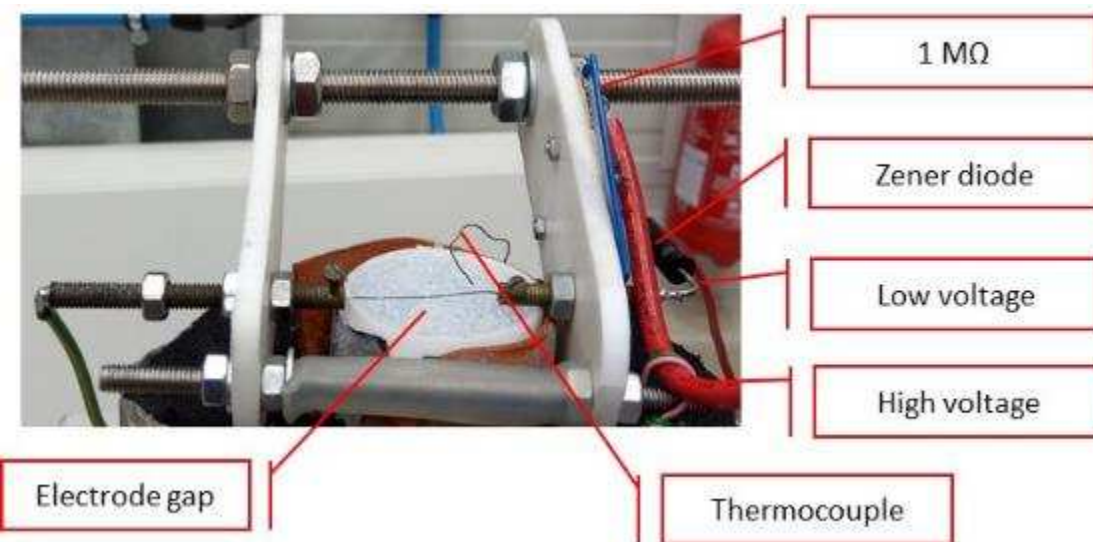


Figure 11: Spark gap arrangement

As for the spark generator, a large variety is described in the literature. An electrical spark is a two steps process. During the “disruption phase”, a large voltage is required (typically 3000 V/mm) to ionize the atmosphere and create a “streamer” (ionized canal visible on figure 11). The current remains very low during that phase (micro amperes). After, the “arc” starts during which a large current is allowed to flow through the spark gap which behaves somewhat as a thermistance. The voltage amounts a few volts to several tens of volts which currents amounting tens of Amperes. In many spark generators, the electrical energy is stored in a single capacitor and is used to create the disruption and the arc. Sometimes the capacitor is charge under a moderate voltage and discharged into a transformer to increase the voltage. Electrical losses are enormous, the spark/stored energy being as low as 1%. To obtain a better yield, a direct capacitor discharge should be used with a much-reduced length of cable to diminish the global impedance (inductance, resistance). This is what was done in the present work.

If a purely capacitive circuit was used with a few meters of cables, the expected resistance would be a fraction of 1 ohm and the inductance nearly zero. Using a single high-voltage capacitor and a 0.5 mm spark gap, a minimum voltage of 3000 V would be required meaning a typical capacitor value of 5 pF (this is much too low in practice) to be able to deliver 10 μ J. The energy is dissipated into the resistances within a time scale amounting $R.C = 10^{-12}$ s which is much too short. This is the reason why it is suggested, in the standards for instance, to add a rather large inductance (1 mH). Its role is to increase the impedance of the circuit without consuming much energy (which a resistor would do). The disadvantage is certainly that the voltage and current signals are more complicated.

In practice, using and controlling such a circuit is difficult, because of the very low capacitance and because of the necessity to use a contactor which will not dissipate the energy. Our trials confirmed this point and this technique was rapidly abandoned.

So, it was decided to disconnect the two phases of the spark. A separate high voltage and high impedance circuit is used to produce the streamer. A second, low voltage and low impedance circuit, is used to produce the arc and dissipate the energy. The high voltage current is delivered through a set of 7 resistors (1 G Ω each) limiting the current supplied by the generator to about 1 μ A. The low voltage current is delivered through a set of 11 resistors (1 M Ω each) offering the possibility to produce continuous sparking at a rate of about 10-100 Hz. A 1 mH coil is in series. A Zener diode prevent the high voltage to be transmitted to the low voltage circuit. The contactor is on the high voltage circuit. Once the streamer is created the low voltage circuit discharges automatically. The circuit is presented on figure 12 (slightly simplified from that shown in the appendix). The current is measured using a standard current gauge (torous) and the voltage with a high voltage probe.

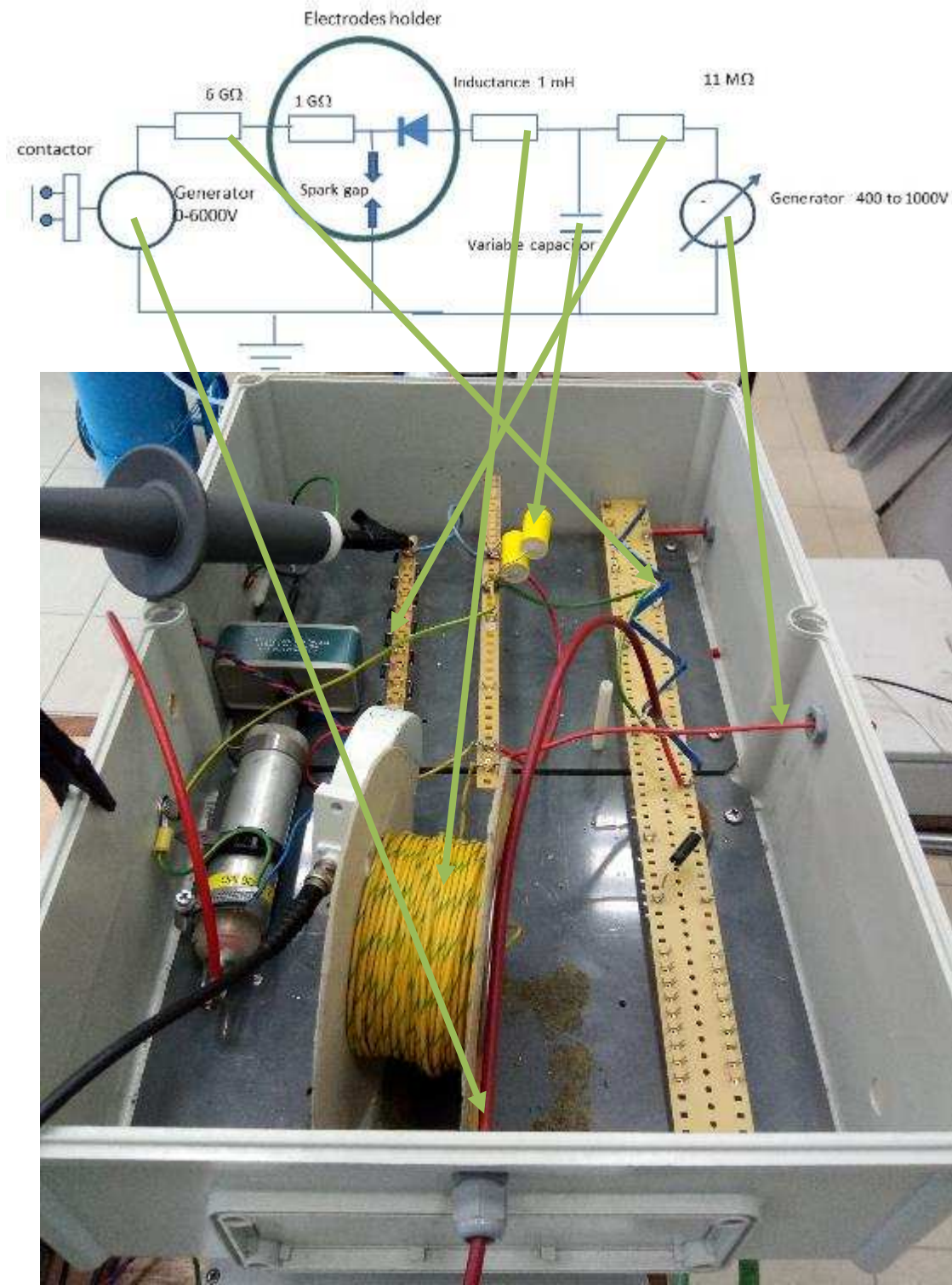


Figure 12: Scheme and photograph of the electrical circuit

The spark gap and the Zener diodes being short-circuited, the total capacitance of the low voltage part of the circuit is that of the charge capacitor. A residual value of 5-10 pF constituted by the high voltage probe exists. If no coil is added, the inductance is $1.7 \mu\text{H}$

and the resistance is 0.1Ω . With the coil inserted, the inductance is 1 mH and the resistance is 2Ω . Because of the high voltage required to trigger the arc, any capacitance on the high voltage side of the circuit may store and add a significant amount of energy to the spark (as estimated above) under the form of a tiny precursor spark. It was in particular measured that a 1 m -long high voltage cable amounts about 20 pF which is much too large (energy stored = $90 \mu\text{J}$...). To remove this difficulty an extra resistor is added as close as possible to the spark gap, on the electrode holder (figure 11). However, observation revealed that very tiny sparks occurred even when the low voltage circuit was not charged (figure 13). This means that a residual capacitance remained. The high voltage circuit and the Zener diode are responsible for this. The residual capacitance had to be estimated. To do this, the frequency of the sparks was measured at different voltages ($4000, 5000, 6000 \text{ V}$) and under different configurations : as it stands, Zener diode disconnected, with reference capacitors added in parallel on the spark gap (2.5 and 7.7 pF). Under the realistic assumption that the breakdown voltage in the air of the laboratory was constant during the measurement, it was found that the residual capacitance of the high voltage circuit is only 1 pF and that of the diode is 3 pF so, 4 pF in total. The breakdown voltage for the 0.5 mm gap in the air of the laboratory was about 3000 V . It was verified that these precursor sparks are not able to ignite any hydrogen air mixtures.



Figure 13: High voltage spark alone (left) and low voltage spark (right)

During the experimental campaign, the high voltage value was hardly varied and fixed to 5000 V . Note that a much lower value may have been chosen since the breakdown occurred typically around 3000 V . But the frequency of the spark depends on the high voltage value. At 5000 V , this frequency is about 40 Hz , which was judged correct (the charging time of the low voltage capacitor is at most 0.01 s , corresponding to 100 Hz). Note that this high voltage is never reached since the breakdown occurs at about 3000 V .

Further testing was performed to investigate the low voltage part behavior. The high voltage part was first disconnected to limit the noise affecting the very beginning of the signal at the start of the breakdown. The discharge was obtained by short-circuiting manually the electrodes. When the diode is removed and when the 1 mH coil is removed too (figure 14), a short spark is produced during some microseconds. Note this duration is in the optimum range for MIE measurements but the current is very large likely to cause significant Joule losses.

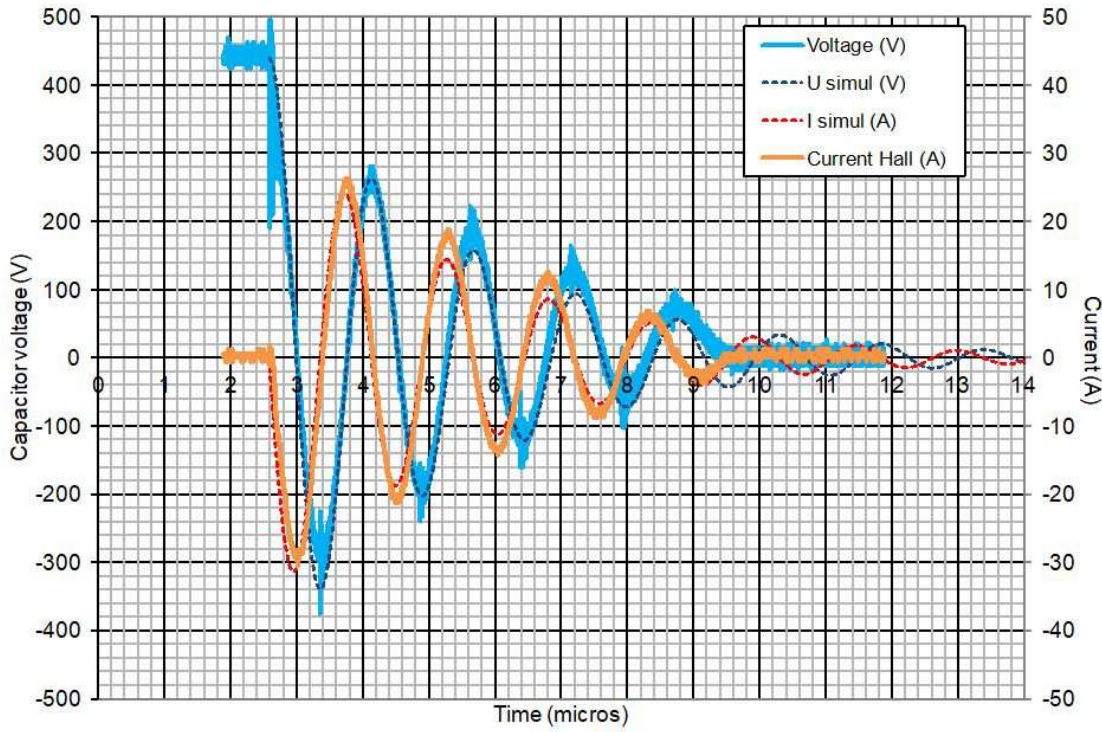


Figure 14: Current voltage signals : no streamer, manually triggered spark, without additional inductance, 440 V in the 20 nF capacitor, without the diodes.

In the second test, the diodes were reintroduced (figure 15).

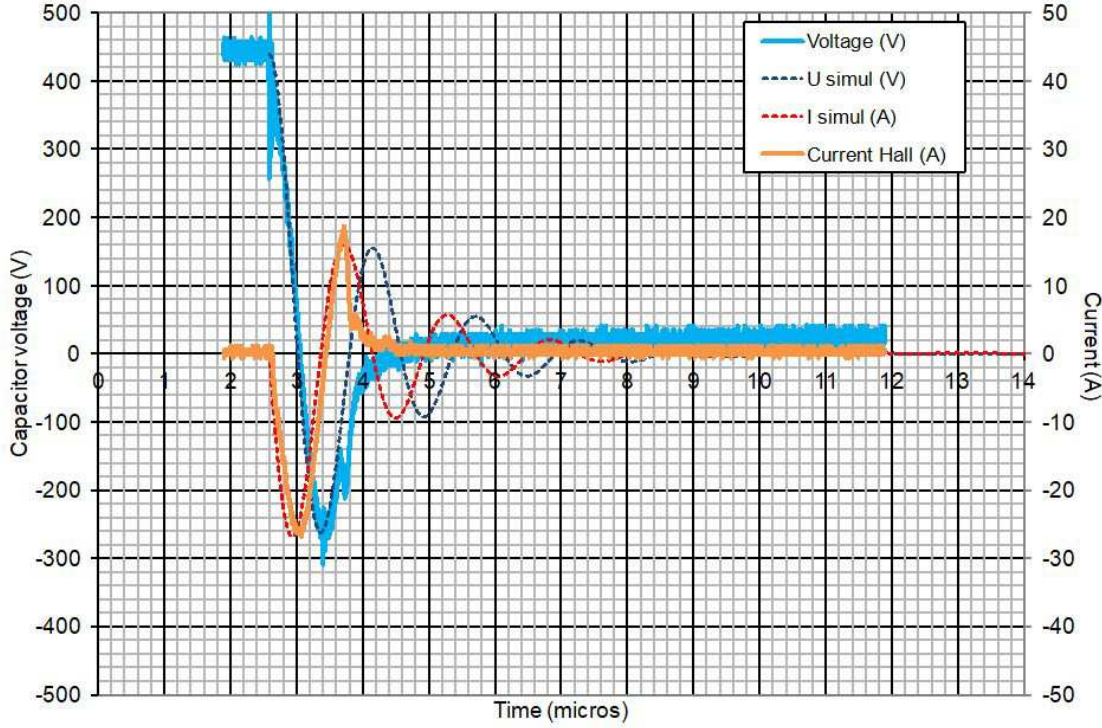


Figure 15: Current voltage signals : no streamer, manually triggered spark, without additional inductance, 440 V in the 20 nF capacitor, with the diodes.

The damped oscillating signal of figure 14 is typical of RLC circuits with a small resistance. Clearly, the diodes have a strong influence (figure 15) and remove a lot of energy. A simulation of the RLC circuit was performed (appendix 2), and the results are the dotted lines on figures 14 and 15. It turns out that the best fit is obtained with an inductance of $3 \mu\text{H}$ (capacitor=20 nF) and a resistance of 2Ω for figure 14 and an inductance of $3 \mu\text{H}$ (capacitor=20 nF) and a resistance of 4Ω for figure 15. When the diode is short-circuited, it can be verified that all the energy is consumed in the resistance. The latter is much larger than the natural resistance of the wires and charge resistor as measured initially (0.1Ω). Most probably then it is that of the spark gap. When the diode is incorporated, the best fit is obtained with $R=4\Omega$ at least until about $3.5 \mu\text{s}$. After this, a catastrophic change appears suggesting a strong increase of the resistance as the Zener diode starts to open the circuit. The characteristic of the circuit turns from a LC to a RC dominated. In terms of energy, the average resistance needed to close the balance would be 6Ω . It means that about half of the energy is dissipated in the spark gap.

Similar measurements were performed with the complete circuit, meaning with the streamer and the 1 mH inductance (added resistance= 2Ω). The voltage is measured at the spark gap. The signals (figure 16) resemble that of figure 15 but over a larger timescale ($10 \mu\text{s}$ instead of 1) as expected. This is still in the optimum range for MIE measurements. The very beginning of the current signal is an artifact probably due to the Zener diodes closing the low voltage part of the circuit. The simulation shows that the best fit is obtained with $L=0.4 \text{ mH}$ (instead of 1 mH) and $R=150 \Omega$. This value of the resistance closes the energy balance as well. This increase of the resistance as compared to figure 15 is due the spark gap which resistance increases when the current intensity decreases. In such a situation with a reduced current, the yield is better, up to 90%.

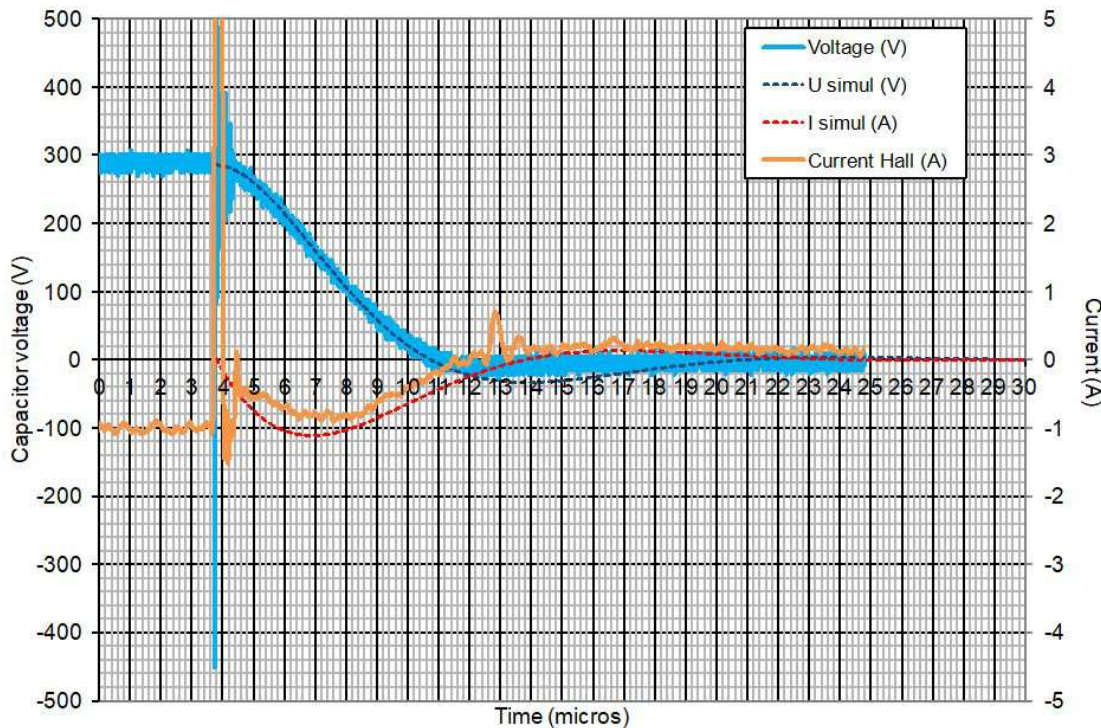


Figure 16: Current voltage signals: streamer triggered spark, with a 1 mH additional inductance, 290 V in the 20 nF capacitor, with the diodes.

Using this kind of modelling, it is possible to estimate the electrical energy dissipated in the spark gap. Many experiments were done and some examples are shown in Appendix 2. Such experiments showed that it is possible to calculate the yield of the spark by fitting the current curve with the measured one. To do this, the resistance of the spark gap is adjusted. The energy dissipated in the spark gap during the first pulsation (after the Zener diode opens the circuit) is calculated and compared to that stored initially in the low voltage capacitor. The yield estimated by this method is close to that measured (via the integration of the I-U signal at the spark gap).

Some relationship between the resistance of the arc and the current through it was obtained : $130\ \Omega$ at $0.8\ A$, $100\ \Omega$ at $1.5\ A$, $60\ \Omega$ at $2.5\ A$, $35\ \Omega$ at $4\ A$ and $5\ \Omega$ at $20\ A$. using this information it is possible to estimate the yields in the conditions of the present experimental campaign.

In the ignition tests, the low voltage capacitance was varied between 10 and $1000\ pF$ with the majority approximately $100\ pF$. The low voltage value ranged between 400 and $1000\ V$. Using and average spark gap resistance during the arc on the order of $150\ \Omega$ and taking $L=0.4\ mH$ as suggested above, it is found, that the maximum current is between $0.1\ A$ and $1\ A$. The yield is about 50% . A similar estimate is attempted for the high voltage circuit. The typical duration of the spark is certainly a fraction of microsecond (typically $10^{-7}\ s$) as suggested by the rapid oscillations on the voltage signal on figure 15 which are due to the high voltage spark. The intrinsic inductance is presumably on the order of $1\ \mu H$. It is found that the maximum current is $5\ A$ and the spark resistance may amount $30\ \Omega$. The yield of the high voltage spark is about 20% .

3.3 MIE measurements

A long investigation was performed with hydrogen air mixture at ambient temperature. As shown on figure 10 above, hydrogen and air are delivered from bottles. Air is “synthetic” containing $20.9\% O_2$ and the rest in N_2 . Nearly no humidity ($400\ ppm$).

While performing a MIE search, it is important to start from the ignition side. It is known by experimentalists that the ignition may differ considerably when starting from the no ignition zone. MIEs are much higher. The reason is unclear but perhaps the combustion cleans up or chemically activates the tip of the electrodes.

The results are presented on figure 17. Note that the energies are those stored in the capacitors (high and low voltage). The yield is not introduced. To calculate the high voltage spark energy, the voltage breakdown was measured and is $2700\ V$ in the air of the bottle at ambient temperature and atmospheric pressure. The values are in line with the data from the literature (see deliverable 4.1) with a minimum at 20% amounting $18\ \mu J$. Little overlap between the no ignition zone and the ignition zone (a factor 2) is much better than in previous studies (with a decade overlapping). This shows that the ignition process is more deterministic than usually claimed. The present authors think the accuracy might be further improved.

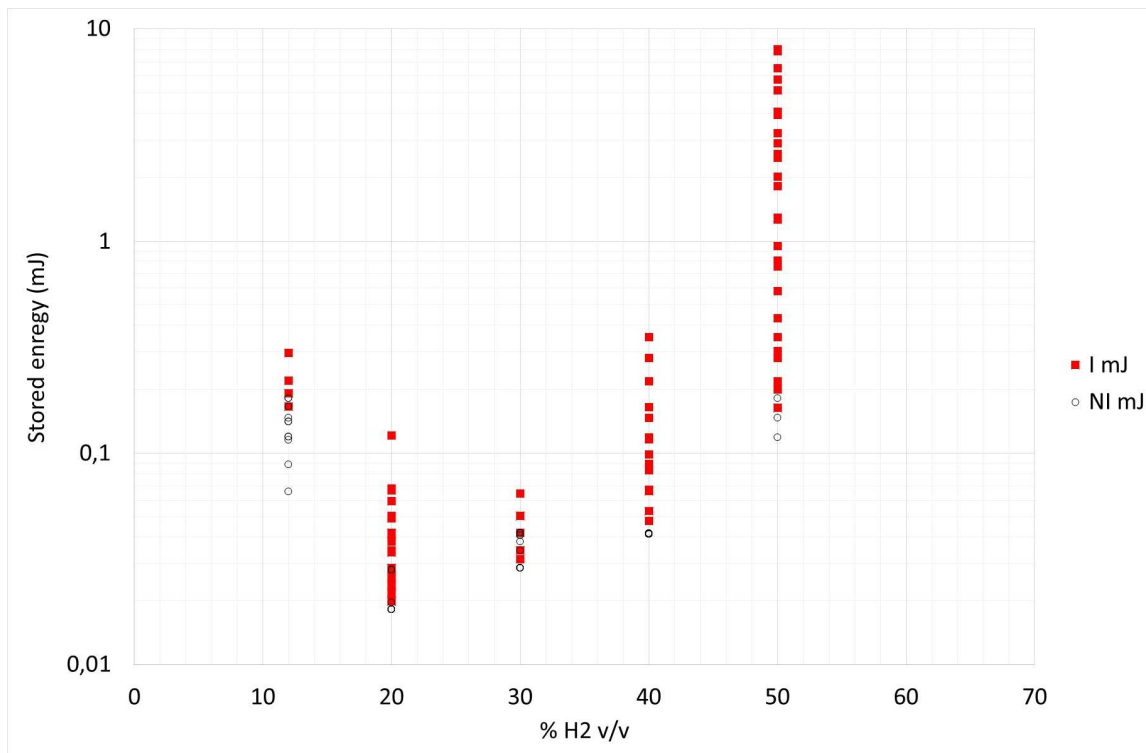


Figure 17: MIE for hydrogen-air mixtures at ambient temperature and atmospheric pressure

Similar measurements were done at about -100°C. The breakdown voltage in the air of the bottle and at atmospheric pressure is 3500 V. Results are presented on figure 18. Tests are more difficult to do and the results are less accurate. Nevertheless, the minimum is found for 20% H₂ and the MIE is larger about 50 µJ.

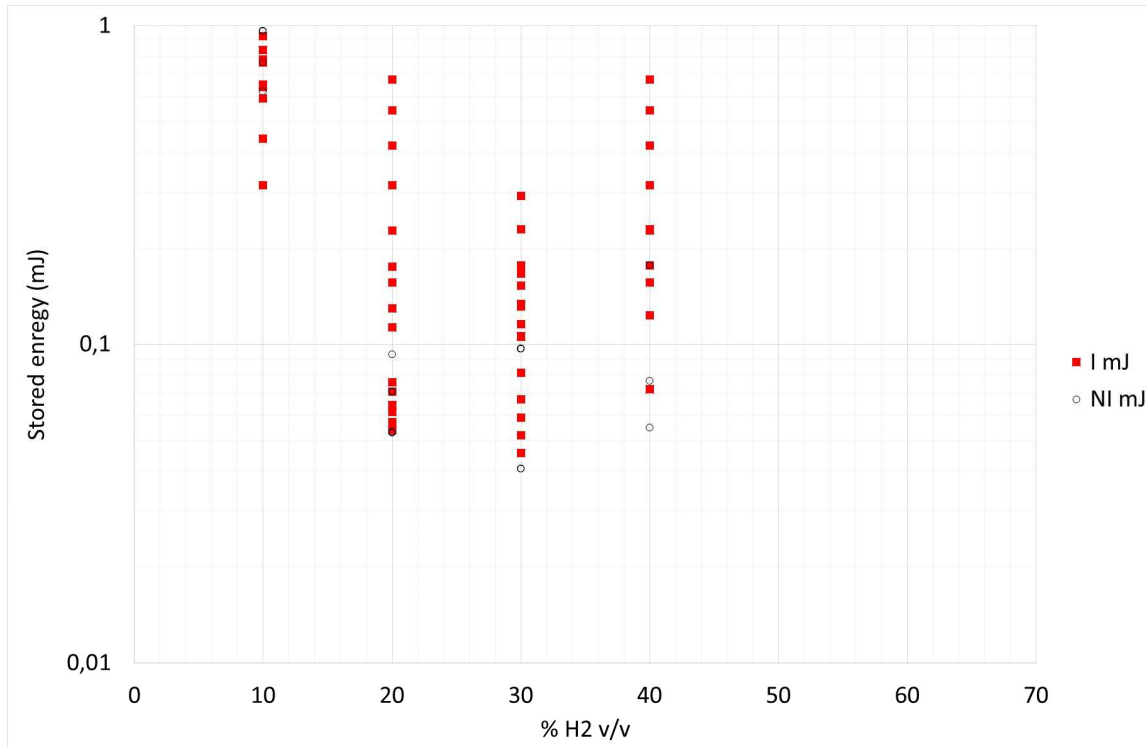


Figure 18: MIE for hydrogen-air mixtures at -100°C and atmospheric pressure

A more systematic investigation of the evolution of the MIE as function of the temperature for the optimum composition (20% H₂) was performed. First, the breakdown voltage variation (in the dry air of the bottle) was needed (figure 19). The latter increases as the temperature drops.

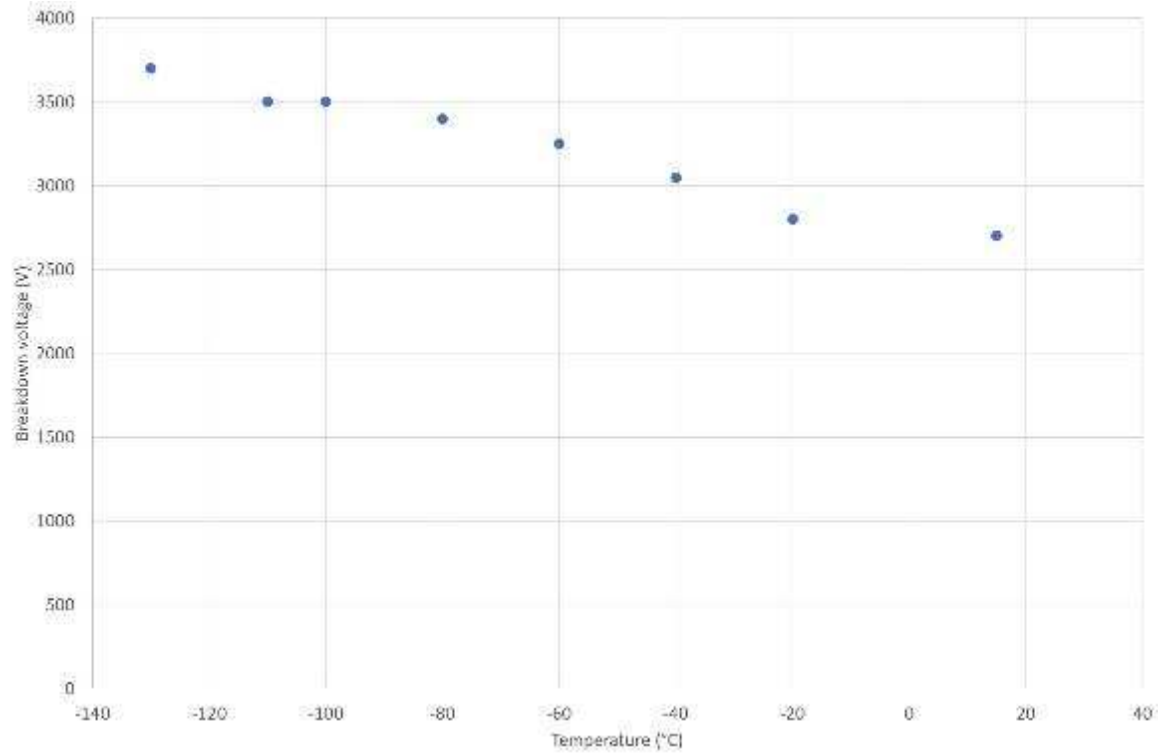


Figure 19: Breakdown voltage in the air of the bottle as function of the temperature at atmospheric pressure.

Figure 20 presents the evolution of the MIE of 20%H₂-air mixtures as function of the temperature. The increase of MIE does not seem linear.

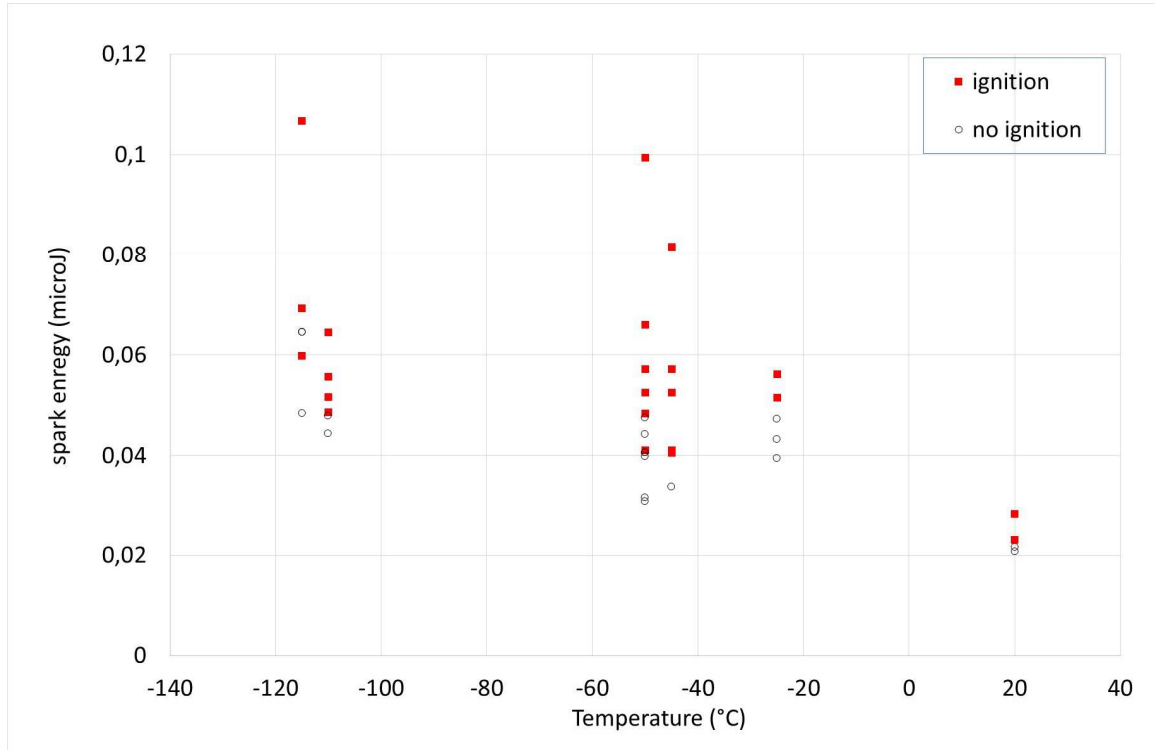


Figure 20: MIE of 20% H₂-air mixtures as function of the temperature at atmospheric pressure.

3.4 LFL-UFL measurements

The spark system was used to find the flammability limits of H₂-air mixtures when the temperature drops. A very large energy of mJ was chosen (64 nF under 800 V) which was judged enough for those mixtures according to the literature.

The flame cannot be seen by eye and the ignition process is silent. To detect the flame an infrared camera (FLIR) was used. The results are presented in table 1.

Temperature (°C)	LFL (% H ₂ v/v)	UFL (% H ₂ v/v)
20	5	70
-60	5.6	66
-120	6	60

Table 1: LFL/UFL of H₂-air mixtures as function of the temperature at atmospheric pressure

4 Conclusions

In this paper, two new experimental systems to produce hydrogen-air mixtures at cryogenic temperatures are described.

The first one devoted to the measurement of the hot surface ignition temperature is a straight tube producing flowing since the ignition temperatures was expected to depend on the flow velocity. Experiments could be performed down to -150°C at atmospheric pressure and up to 25 m/s flowing velocity. The hot surface is a nichrome coil wired around an

alumina core (9 mm diameter, 30 mm long). Surprisingly, the ignition temperature does not depend on the temperature nor on the velocity of the mixture. It hardly depends on the concentration of hydrogen. The minimum value of the hot surface ignition temperature is little less than 600°C for 10% H₂ v/v. Note this value is close to the autoignition temperature of hydrogen air mixtures suggesting the ignition mode around a heated rod is similar. This is perhaps a specificity of hydrogen air mixtures.

To measure the MIE a refrigerated burner was designed. It is a 40 mm diameter, 40 cm high column filled with glass beads. The mixture is fed from the bottom and the spark gap is located at the top. To cool down the mixture the glass beads are cooled before the test by pouring about 2 litres of liquid nitrogen. Experiments could be performed down to -140°C (atmospheric pressure) this way. This burner can be used to measure most of the fundamental combustion parameters of such mixtures : minimum ignition energies (MIEs), flammability limits, laminar burning velocities. To measure the MIE a new type of spark generator was produced offering the possibility to control rather accurately the energy delivered to the spark.

A considerable effort was devoted to the measurement of MIEs. Although some uncertainty remains, the ignition and no ignition zone overlap is very significantly reduced as compared to other equipment. Nevertheless, some variability remains probably due to the electrodes. When decreasing the temperature, the minimum ignition energy (at 20% H₂) increases slightly from about 20 µJ at 20°C, to 40 µJ at -50°C and 50 µJ at -120°C.

The flammability limits were estimated using the same burner method when the temperature drops. A very high spark energy was chosen (20 mJ). As expected, the flammability domain diminishes.

Appendix 1: first version of the MIE device

The explosion chamber is a 7-liter transparent cylindrical chamber (figure A1) able to support a static internal pressure amounting 100 bars. It is equipped with a number of measuring ports and feeding lines.



Figure A1: Explosion chamber (bottom : 200 mm ID and 200 mm high)

The mixture is prepared into a small stainless-steel mixing tank (0.1 l) using mass flowmeters (figure A2). The composition is controlled using a paramagnetic oxygen meter (SERVOMEX : O₂% accuracy = $\pm 0.01\% \text{ v/v}$) upstream of the chamber and downstream to control that the chamber is correctly filled. For a targeted 5% v/v fuel/air mixture, the accuracy of the composition is : $5 \pm 0.1\% \text{ v/v}$.

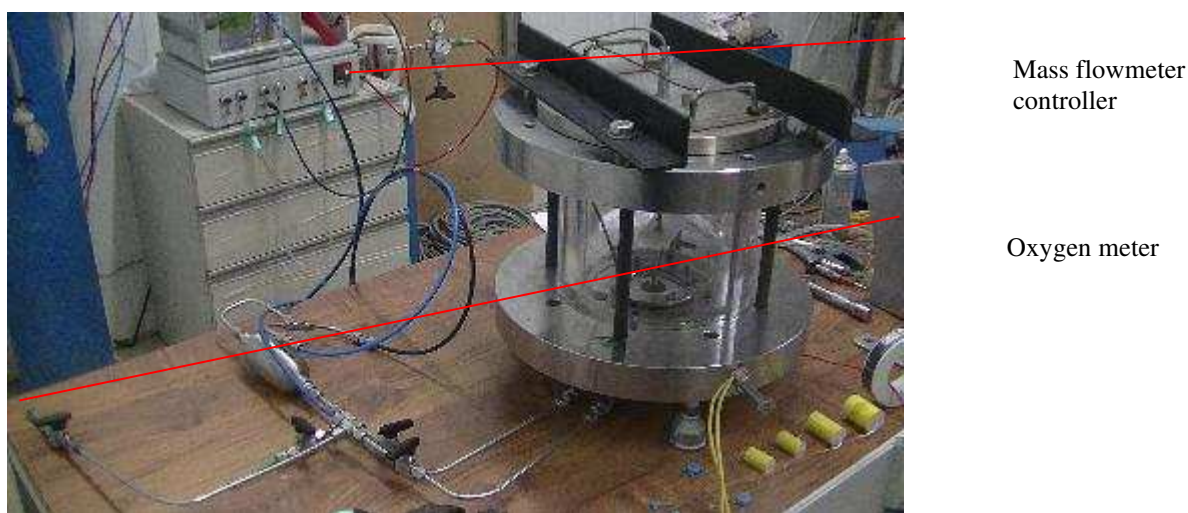


Figure A2: Mass flowmeter arrangement for propane-air experiments

The maximum explosion (over)pressures are measured using a Kistler 10 b piezoresistive gauge. High speed video (up to 10000 fps: Photron camera) is used to offer a possibility to control the MIE measurement by using the correlations presented in the deliverable D4.1.

The spark gap layout is shown on figure A3. The electrodes are 0.1 mm in diameter (Tungsten) tightly screwed on steel rods in such a way that any heat loss sources (supports, walls) are 10 cm away from the spark gap.

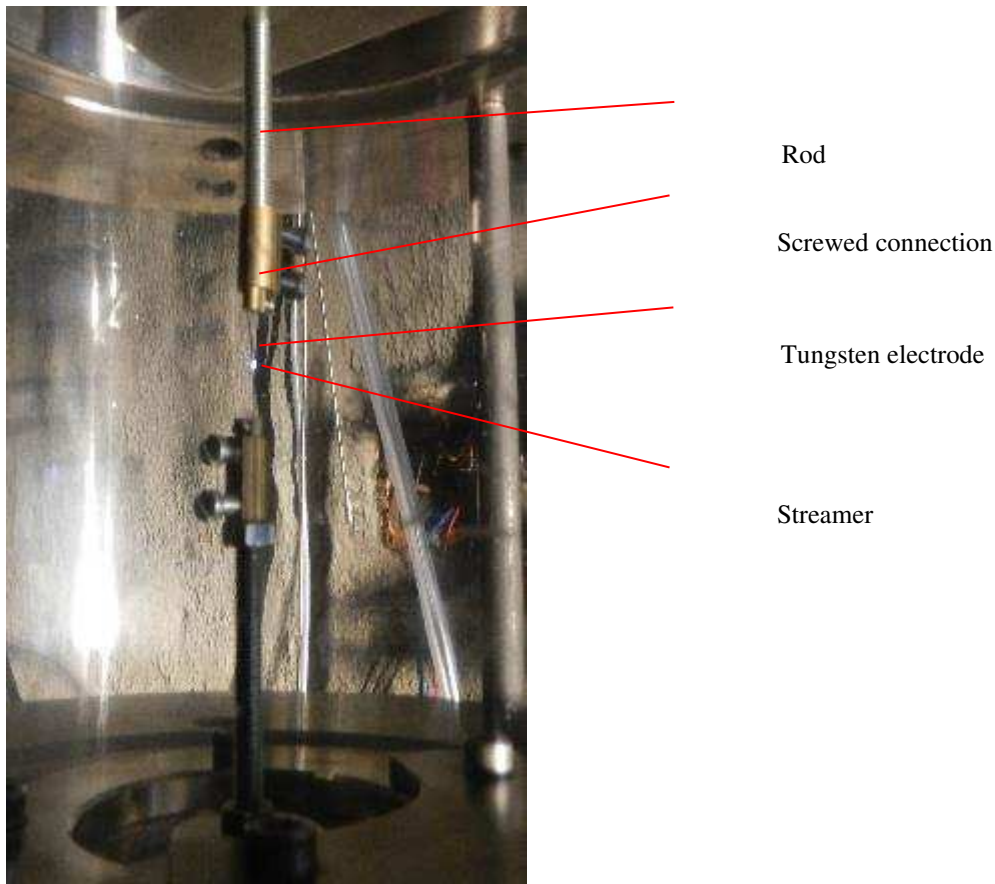


Figure A3: Spark gap arrangement

As for the spark generator, it was decided to disconnect the ionization phase of the spark from the arc phase. A separate high voltage and high impedance circuit is used to produce the streamer. A second, low voltage and low impedance circuit, is used to produce the arc and dissipate the energy. The contactor is on the high voltage circuit. Once the streamer is created the low voltage circuit discharges automatically. A set of Zener diodes prevents the high voltage to be transmitted to the low voltage circuit. The circuit is presented on figure A4. The current is measured using a standard current gauge (based on the principle of the Hall effect). As it stands, the spark gap and the Zener diodes being short-circuited, the total capacitance of the circuit is 20 nF (charge capacitor but which can be varied depending on the mixture), the inductance is 1.7 μ H and the resistance is 0.1 Ω . The measured capacitance of the chamber, of the diodes and of the high voltage cable is not more than 45 pF, half of this being due to the cable.

The additional 1 mH inductance is placed close to the electrodes. It is not inside the spark generator box but outside since it can be removed or modified. The main advantage of the device is that the stored energy can be varied in very large proportions since it was verified that an arc is produced down to voltages as low as 35 V. In theory, the stored energy can be varied between 10 and 2000 μ J without changing the capacitor. Note that it was verified that the streamer is not able to ignite the mixture.

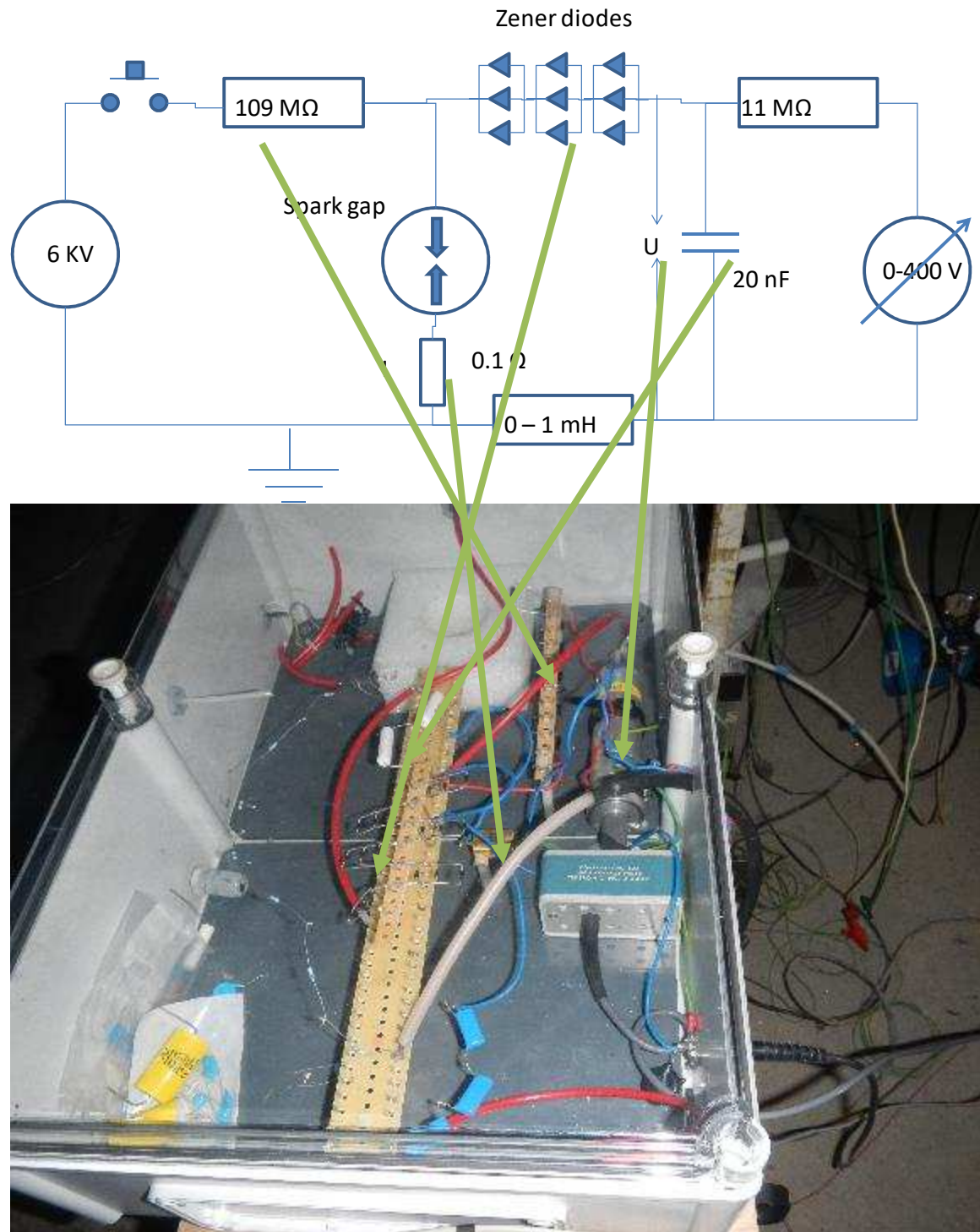
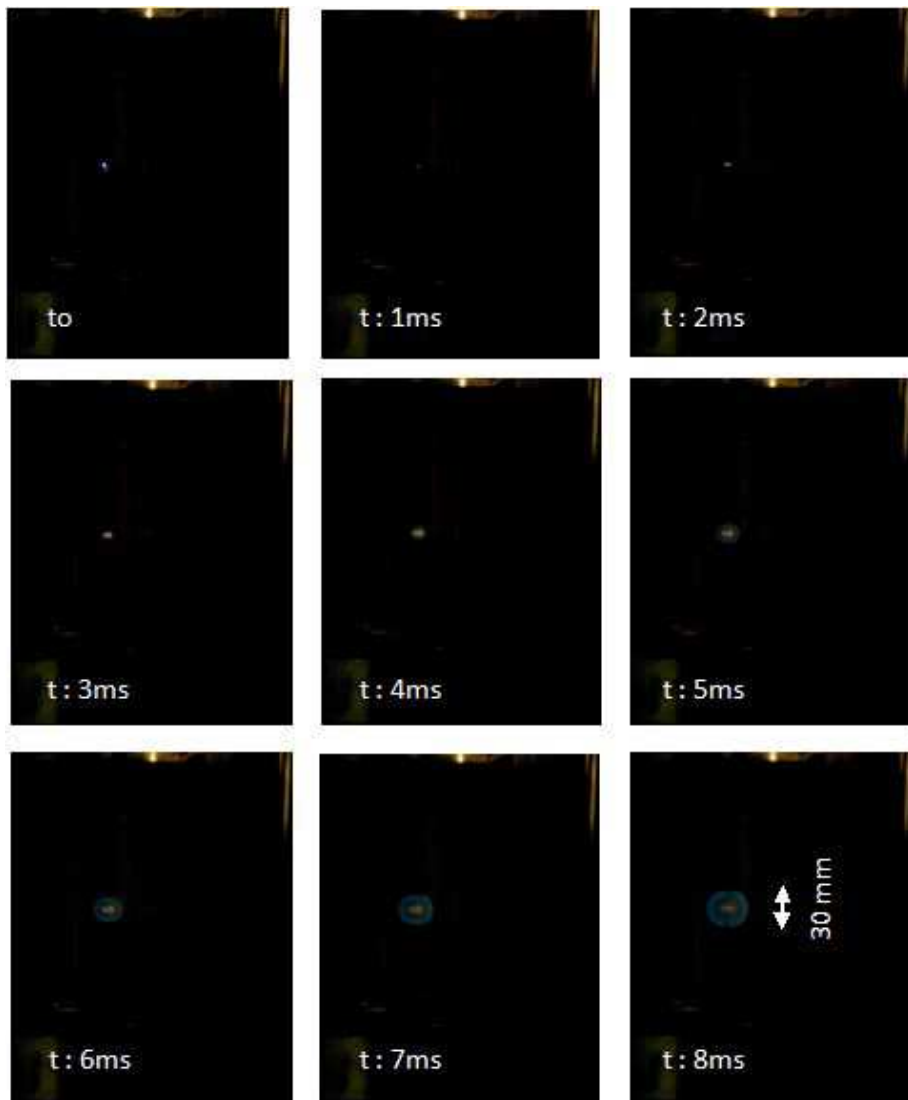


Figure A4: Scheme and photograph of the electrical circuit

Propane air tests were performed first.

A typical sequence is shown on figure A5. A double lobed structure appears just after the spark which seems to be double vortex and would suggest a Maecker effect due to the flow of heavy ions between the electrode. This “jet” is mostly responsible for the energy transfer between the spark gap and the mixture. After, a blue flame kernel is formed expanding out. The expansion velocity is a few m/s.



FigureA5: Flame kernel development (4.5% C₃H₈ in air, 400V, 1 mH)

The minimum ignition energy measurements are shown on figure A6. The values are three quarters the energy stored in the capacitor to account for the losses. The voltage is dropped gradually until systematic no ignition. Each test is repeated 10 times. There is some overlap between the no ignition zone and the ignition zone which is rather common in such tests and may result from the development of the flame kernel and may be of some uncertainties about the exact composition of the mixture.

Similar raw data from the literature¹ are presented on figure A7 for comparison. The present results appear in good agreement with the available data.

¹ Moorhouse, J., William, A. and Maddison, T.E (1974): An investigation of the minimum ignition energies of some C1 to C7 hydrocarbons. Combustion and Flame, vol. 23, pp. 203-213.

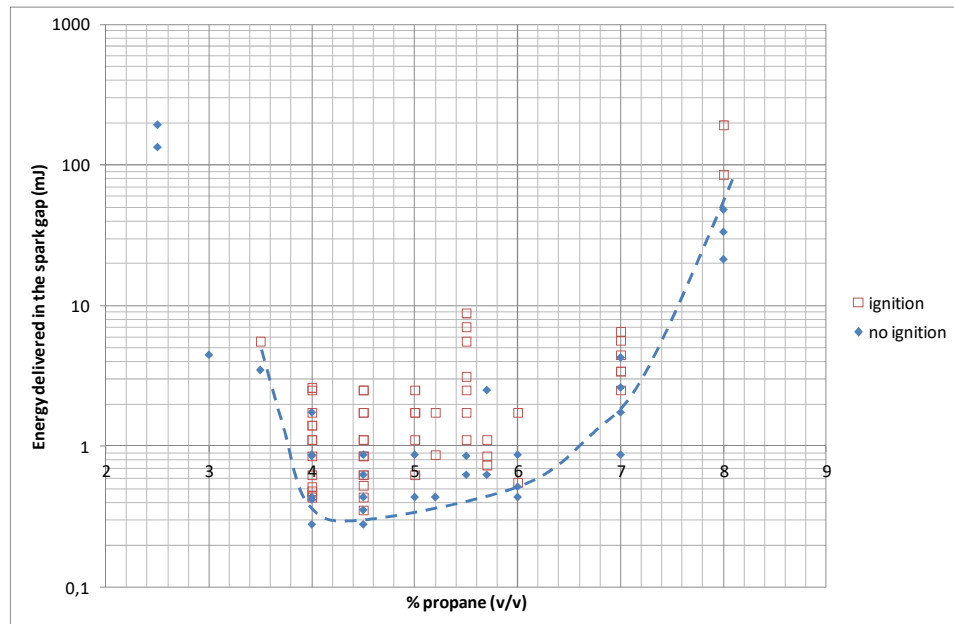


Figure A6: Minimum ignition energies for propane air mixtures at ambient conditions

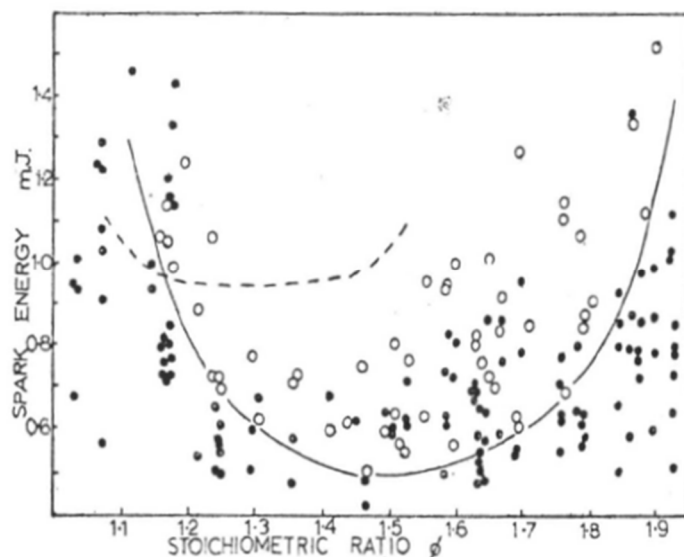


Figure A7: Data from the literature about the minimum ignition energy of propane-air mixtures at ambient conditions

In addition, some tests with hydrogen-air mixtures were done at ambient conditions. The results are shown in figure A8 and A9 showing a promising future.

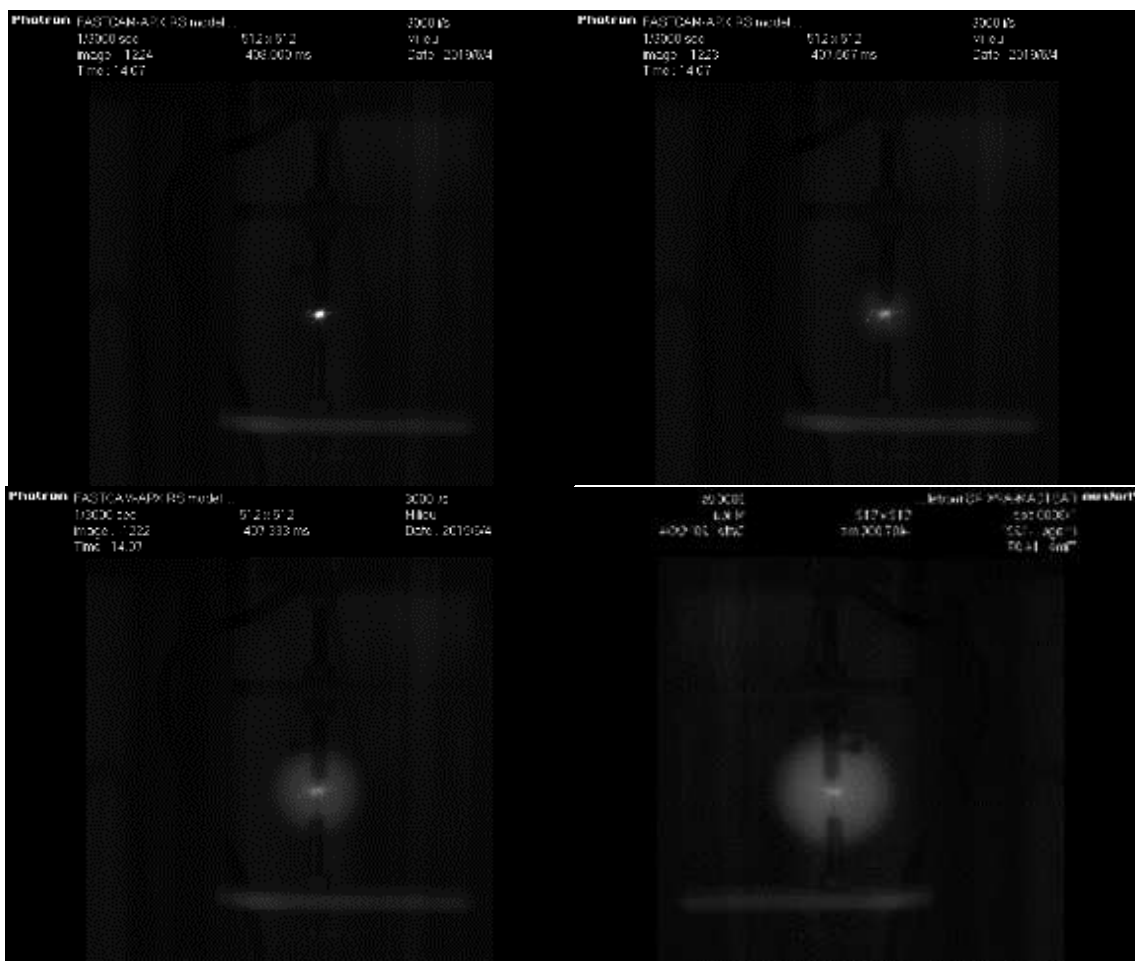
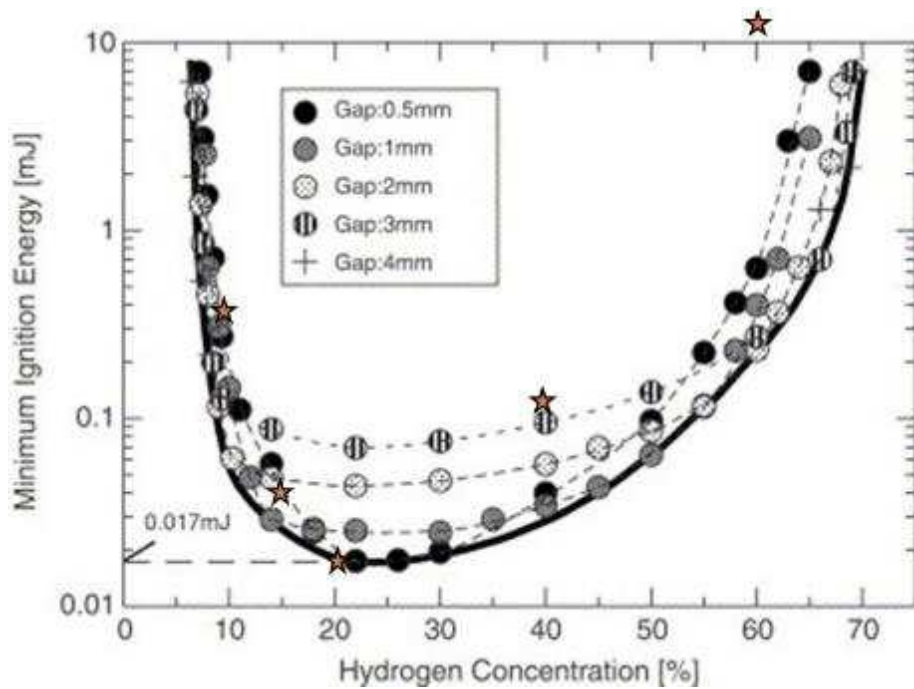
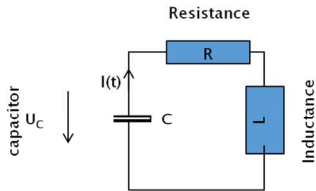

 Figure A8: Flame kernel development (40% H₂ in air)


Figure A9: Minimum ignition energies for hydrogen air mixtures at ambient conditions (present results are the stars together with data from the literature see deliverable D4.1)

Unfortunately, several difficulties condemned this route. First, a lot of water vapour is produced during a successful ignition. Humidity is trapped on each insulating surface which drains currents so that sparking at low energy becomes impossible. The vessel needs to be open carefully dried and closed again which represent a considerable amount of work. Second, it proved nearly impossible to cool down the vessel to -100°C and maintain it at this temperature for a long enough time. Materials become brittle and tightness cannot be insured. Because of this the burner method was developed.

Appendix 2: spark yield

R,L,C model (i)



$$I(t) = -\frac{Q_0}{\sqrt{L \cdot C}} \cdot \frac{1}{\sqrt{1 - \frac{R^2 \cdot C^2}{4}}} \cdot \sin\left(\frac{t}{\sqrt{L \cdot C}}\right) \cdot e^{-\frac{R \cdot t}{2 \cdot L}}$$

$$Q_0 = C \cdot U_{C_0}$$

- As shown hereafter, only the first pulse is detectable when Zener diodes are placed on the circuit.
- T the duration of the pulse
- Optimisation of the circuit fitting L, C and R on the real curves

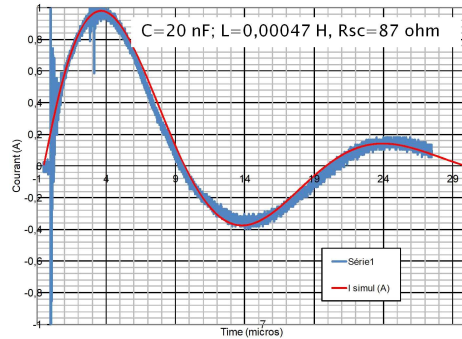
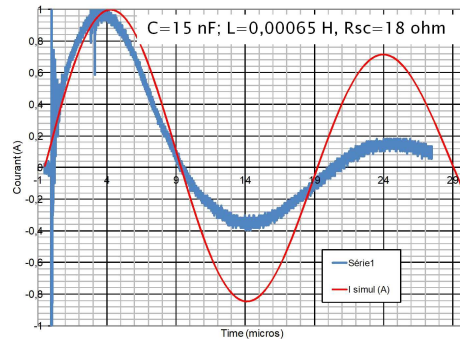
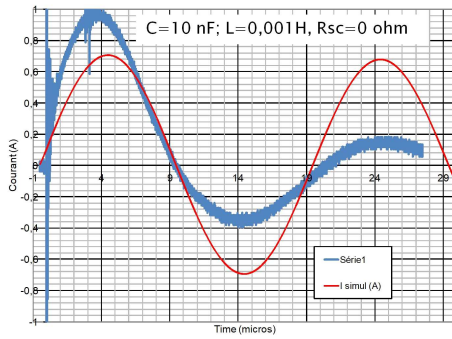
$$\omega_{oscillation} = \frac{1}{\sqrt{L \cdot C}} = \frac{2 \cdot \pi}{T_{oscillation}} = \frac{\pi}{T}$$

Présentation INERIS – 07/12/2017

6



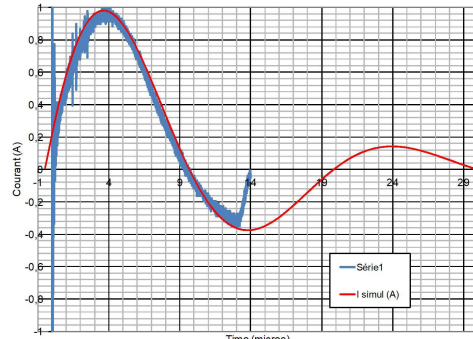
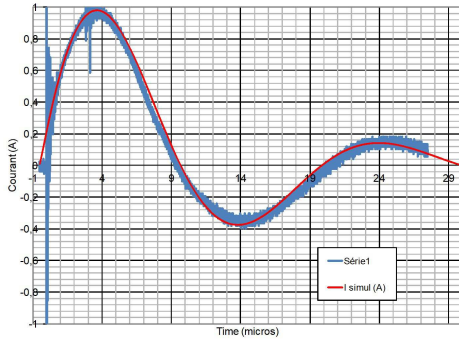
Best fit exercice on test 23 (no ionisation, no diode, short circuit)



Présentation INERIS – 07/12/2017



Best fit exercice on test 25 (no ionisation, with diode, short circuit)

 $C=20 \text{ nF}; L=0,00047 \text{ H}, R_{sc}=87 \text{ ohm}$


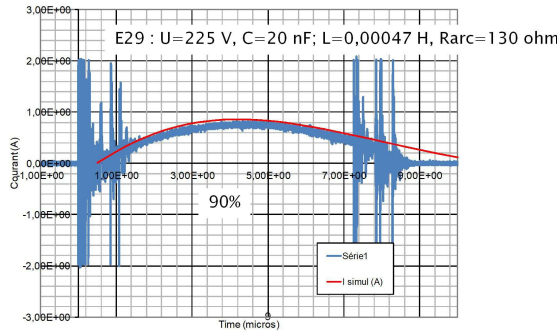
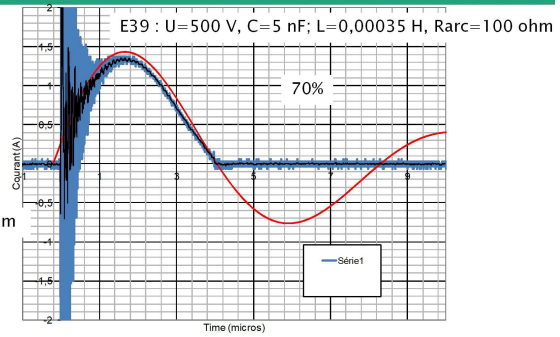
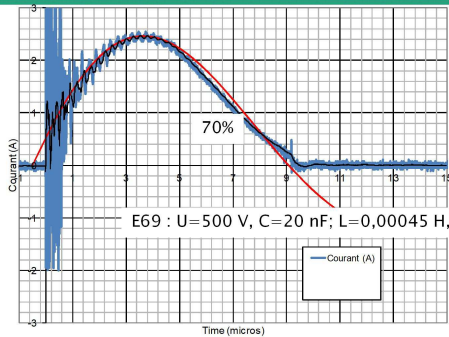
So :

- the capacity of the circuit is the nominal one, but the inductance may be less at high frequency
- The diode does not change that
- To estimate the yield of the circuit the best fit is applied with the nominal capacitor, and an adjusted inductance and arc resistance (the circuit resistance is 2 ohms)

Présentation INERIS – 07/12/2017

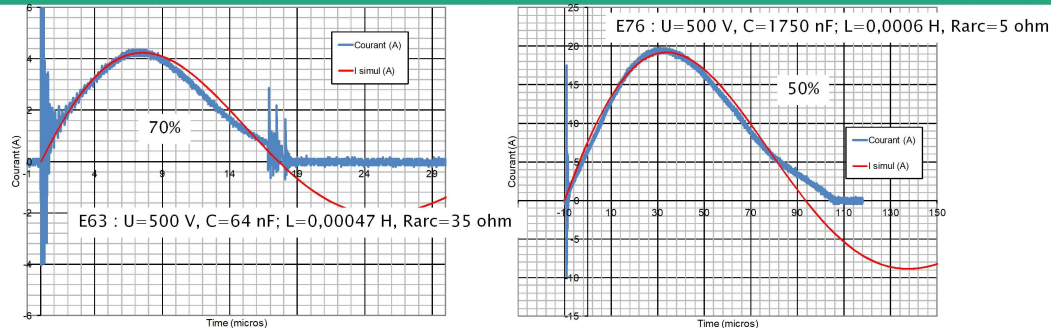
8

Best fit exercice on test 29, E39 (ionisation, diode)



Présentation INERIS – 07/12/2017

Best fit exercise on test 63, E76 (ionisation, diode)



Yield of the circuit (i)

The electrical behaviour of the circuit could be extremely different at high frequency (10 to 100 kHz) than at low frequency (impedances are measured at 1kHz).

Interpreting directly the signal enables a direct estimation of L, C and R from the curve fitting of the theory on the real traces.

The intrinsic resistance of the circuit is about 2 ohm (due to the added inductance).

The best fit is obtained using the nominal capacity but the true inductance is smaller than measured at low frequency. L increases when the duration of the discharge increases confirming the frequency dependency.

In a few instances only, we were able to estimate the voltage across the spark gap and the results are comparable to that estimated via the « fitted » resistance of the spark gap (about 100 V).

The overall yield would be on the order of 70% (energy delivered in the spark gap/stored) and the initial estimate seems then reasonable.

....